Med Chem Res (2015) 24:2645–2655
DOI 10.1007/s00044-015-1316-x

MEDICINAL CHEMISTRY RESEARCH

ORIGINAL RESEARCH

Design, synthesis and in vitro testing of 7-methoxytacrine-amantadine analogues: a novel cholinesterase inhibitors for the treatment of Alzheimer's disease

Katarina Spilovska · Jan Korabecny · Anna Horova · Kamil Musilek · Eugenie Nepovimova · Lucie Drtinova · Zuzana Gazova · Katarina Siposova · Rafael Dolezal · Daniel Jun · Kamil Kuca

Received: 16 February 2014 / Accepted: 29 December 2014 / Published online: 29 January 2015

Abstract A series of cholinesterase inhibitors acting as dual binding site heterodimers for the management of Alzheimer's disease were developed. The series of 7-methoxytacrine (7-MEOTA)-amantadine ureas (**11**–**17**) was designed, prepared evaluated in vitro towards human acetyl/butyryl cholinesterase (*h*AChE, *h*BChE) and compared with the series of 7-MEOTA-amantadine thioureas (**4**–**10**). The heterodimers have different length of linkers combining 7-MEOTA and amantadine moieties. In comparison with 7-MEOTA, the newly synthesized compounds were better inhibitors of both cholinesterases. The urea analogues did not have the anticipated benefit of increased inhibitory activity and have comparable IC_{50} values with thiourea derivatives.

K. Spilovska · J. Korabecny · A. Horova · E. Nepovimova · L. Drtinova · D. Jun
Department of Toxicology and Military Pharmacy, Faculty of Military Health Sciences, University of Defence, Trebesska 1575, 500 01 Hradec Kralove, Czech Republic

K. Spilovska · J. Korabecny · K. Musilek · E. Nepovimova · R. Dolezal · D. Jun · K. Kuca
Biomedical Research Centre, University Hospital, Sokolska 581, 500 05 Hradec Kralove, Czech Republic

K. Spilovska · J. Korabecny
National Institute of Mental Health, Topolova 748, 250 67 Klecany, Czech Republic

J. Korabecny · R. Dolezal · K. Kuca (✉)
Center for Basic and Applied Research, Faculty of Informatics and Management, University of Hradec Kralove, Rokitanskeho 62, 500 03 Hradec Kralove, Czech Republic
e-mail: kamil.kuca@fnhk.cz

K. Musilek · Z. Gazova · K. Siposova
Department of Biophysics, Institute of Experimental Physics, Slovak Academy of Sciences, Watsonova 47, 040 01 Kosice, Slovak Republic

Keywords Alzheimer's disease · Inhibitor · Acetylcholinesterase · Butyrylcholinesterase · Amantadine · 7-MEOTA

Introduction

AD is the most common type of dementia worldwide. It is characterized by a severe and progressive loss of memory (Craig *et al.*, 2011; Jahn, 2013). The prevalence of AD, which increases with age, ranges from 1 to 2 % in the 65 years age group to 35 % or higher in the 85 years age group (Tayeb *et al.*, 2012; Mayeux, 2003). General consensus supports the multifactorial nature of AD with decrease in the neurotransmitter acetylcholine (ACh), formation of amyloid β-protein (Aβ) plaques and abnormal posttranslational modifications of tau protein to yield neurofibrillary tangles. These pathological findings are considered to be closely associated with AD (Tomiyama *et al.*, 1996; Krall and Sramek, 1999; Lahiri *et al.*, 2003; Cummings, 2004; Bartolini *et al.*, 2007; Gauthier and Poirier, 2008).

Most of the currently available compounds intended to treat AD do this by compensating for ACh deficiency and enhancing ACh-mediated transmission (Silman and Sussman, 2005). This is achieved by inhibition of cholinesterases (ChEs) (Giacobini, 2004), a family containing acetylcholinesterase (AChE, E.C. 3.1.1.7.) and butyrylcholinesterase (BChE, E.C. 3.1.1.8.) enzymes that cause degradation of ACh (Darvesh *et al.*, 2003; Greig *et al.*, 2001, 2005; Rizzo *et al.*, 2011; Yiannopoulou and Papageorgiou, 2013). Tacrine, donepezil, rivastigmine and galantamine belong to group of ChE inhibitors (ChEIs) capable of cognitive, functional and behavioural improvement, although none of them proved to be effective against the progression of AD (Fig. 1) (Zemek *et al.*, 2014). Tacrine (9-amino-1,2,3,4-

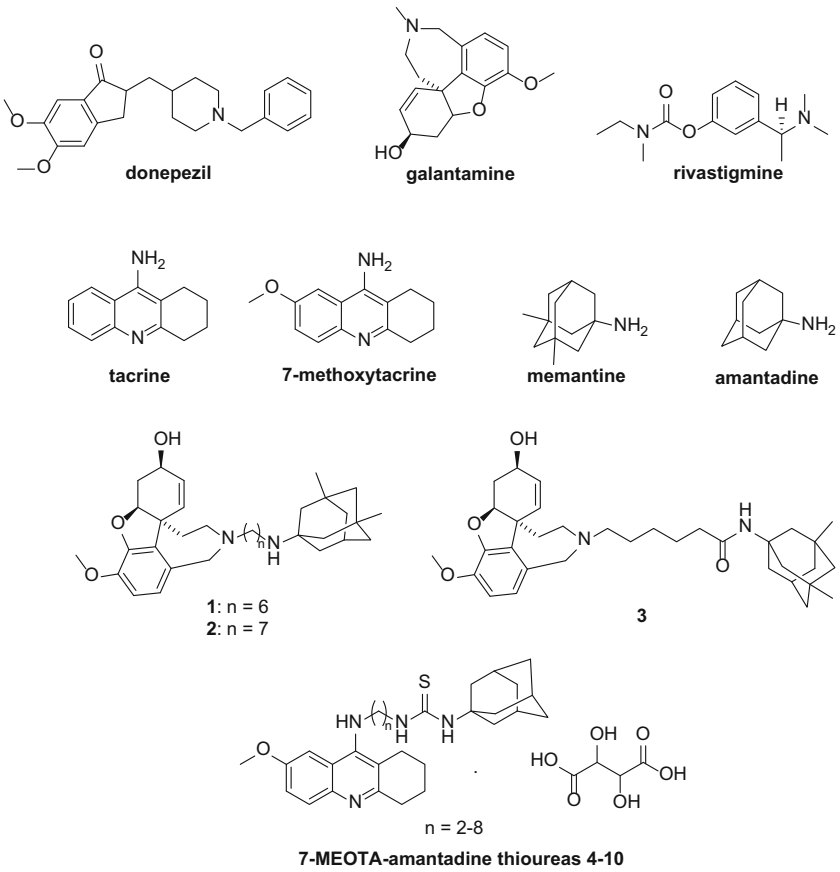

Fig. 1 Structures of ChEIs, derivatives of tacrine, polycyclic amines and 7-MEOTA-amantadine thioureas **4**–**10**

tetrahydroacridine, THA) was the first ChEI approved for the treatment of AD. However, tacrine was withdrawn due to hepatotoxicity (Dejmek, 1990; Summers *et al.*, 1989; Patocka *et al.*, 2008). The 7-methoxy derivative, 9-amino-7-methoxy-1,2,3,4-tetrahydroacridine (7-MEOTA, Fig. 1), was found also to be effective and less hepatotoxic ChEI (Soukup *et al.*, 2013; Marx, 1987; Korabecny *et al.*, 2010, 2011; Korabecny *et al.*, 2014).

Aminoadamantanes (memantine, amantadine, Fig. 1) are used in the treatment of Parkinson's disease (PD) and AD (Caumont and Octave, 2006; Ossola *et al.*, 2011). Memantine is a non-competitive *N*-methyl-D-aspartate (NMDA) glutamate receptor antagonist (Bormann, 1989) approved for moderate to severe AD (Forest Pharmaceuticals Inc., 2003; Manning *et al.*, 2011). Memantine (1-amino-3,5-dimethyladamantane) is used as a neuroprotective agent in the treatment of AD with different mechanism of action (NMDA receptor antagonist) (Kotermanski and Johnson, 2009; Lipton, 2006; Schmitt, 2005). Amantadine (1-aminoadamantane, adamantylamine) is currently used as an antiviral and an anti-PD drug (Blanpied *et al.*, 2005). Amantadine is a weak NMDA receptor antagonist, which is considered to be beneficial for PD and AD patients that need the increase in dopaminergic transmission in order to compensate for the dopamine/glutamate imbalance (Page *et al.*, 2000; Peeters *et al.*, 2002; Magazanik *et al.*, 1996).

Simoni *et al.* (2012) synthesized a novel series of compounds linking galantamine and memantine following the strategy of multi-target-directed ligands (MTDLs). These compounds seem to be effective in treating complex diseases due to their ability to interact with multiple targets responsible for the disease pathogenesis. Selected compounds from this study (**1**–**3**) were found to be capable of inhibiting rat AChE in the nanomolar range. In the MK-801 binding assay against NMDA receptor and against NR2B-containing NMDA receptor (using the ifenprodil binding assay), these dual hybrids showed activity in the micromolar range. Furthermore, neuroprotective profile against NMDA-mediated neurotoxicity was tested using SHSY-5Y cell 5Y cell viability assay and these analogues were found to inhibit NMDA-induced neurotoxicity in sub-nanomolar range (Cavalli *et al.*, 2008; Spilovska *et al.*, 2013; Simoni *et al.*, 2012; Zheng *et al.*, 2014).

Based on the MTDL strategy by Simoni *et al.,* a series of 7-MEOTA-amantadine urea-linked derivatives were designed, synthesized and evaluated as AChE/BChE inhibitors. The design was focused on the compounds development capable of interacting with both the active site

gorge and the peripheral anionic site (PAS) of the enzyme (i.e. a dual binding site inhibitors). These heterodimers were compared with 7-MEOTA-amantadine thioureas, 7-MEOTA, tacrine and galantamine-memantine dimers reported previously (Cavalli *et al.*, 2008; Spilovska *et al.*, 2013; Simoni *et al.*, 2012). The synthetic approach and in vitro ChE inhibition properties are discussed along with molecular modeling studies.

Experimental section

Materials and methods

7-MEOTA was prepared at the Department of Toxicology and Military Pharmacy according to the method described earlier (Pohanka *et al.*, 2008). All reagents were obtained from Sigma-Aldrich in reagent grade quality. All experiments were carried out under nitrogen atmosphere. Thin-layer chromatography (TLC) was performed on aluminium sheets precoated with silica gel 60 F254 (Merck). Column chromatography was performed at normal pressure on silica gel 100 (particle size 0.063–0.200 mm, 70–230 mesh ASTM, Fluka). Elemental analysis was measured at Perkin-Elmer CHN Analyser 2400 Serie II apparatus. Mass spectra were recorded using a combination of high-performance liquid chromatography and mass spectrometry. The HP1100 HPLC system was obtained from Agilent Technologies (Waldbronn, Germany). It consisted of a G1322A vacuum degasser, G1311A quaternary pump, G1313A autosampler and a MSD1456 VL quadrupole mass spectrometer equipped with an electrospray ionization source. Nitrogen for mass spectrometer was supplied by a Whatman 75–720 nitrogen generator. Data were collected in positive ion mode with an ESI probe voltage of 4,000 V. The pressure of nebulizer gas was set up to 35 psig. Drying gas temperature was operated at 335 °C and flow at 13 L/min. ^{1}H-NMR and ^{13}C-NMR spectra were recorded with a Varian S500 spectrometer operating at 500 and 125 MHz, respectively, in deuteriochloroform ($CDCl_3$; 7.27 (D), 77.2 (C) ppm) or hexadeuteriodimethylsulfoxide (DMSO-d_6; 2.50 (D), 39.7 (C) ppm) using tetramethylsilane (TMS) as internal reference (= 0 ppm for both nuclei). Chemical shifts are reported in parts per milion (ppm, δ) relative to TMS. The assignment of chemical shifts is based on standard NMR experiments (^{1}H, ^{13}C, ^{1}H-^{1}H COSY, ^{1}H-^{13}C HSQC, HMBC, DEPT). Melting points were measured on a micro heating stage PHMK 05 (VEB Kombinant Nagema, Radebeul, Germany) and are uncorrected.

General synthetic procedure

In this paper, the required 1-adamantyl-3-(2-(7-methoxy-1,2,3,4-tetrahydroacridin-9-yl-amino)alkyl)urea 2,3-dihydroxysuccinates (**11**–**17**) were obtained via the reaction of early prepared 7-MEOTA-adamantylamine thioureas (**4**–**10**; 10 mmol) with 2,4,6-trimethylbenzonitrile-*N*-oxide (11 mmol) in dichloromethane (5 mL). The reaction mixture was stirred 24 h at room temperature and purified via column chromatography using chloroform/methanol (9:1) as mobile phase. The final products were converted to tartaric salts by the addition of equimolar tartaric acid and stirred in absolute ethanol (10 mL) for 24 h. The final 1-adamantyl-3-(2-(7-methoxy-1,2,3,4-tetrahydroacridin-9-yl-amino)alkyl)urea 2,3-dihydroxysuccinates (**11**–**17**) were obtained as white to yellow powders in good yields.

Experimental procedures and compound characterization

*1-Adamantyl-3-(2-(7-methoxy-1,2,3,4-tetrahydroacridin-9-yl-amino)ethyl)urea 2,3-dihydroxysuccinate (**11**)*

White powder yields 70.8 %; m.p. = 60.4–63.0 °C; ^{1}H-NMR (DMSO-d_6) δ 7.76 (m, 1H, CH, H-5), 7.72 (m, 1H, CH, H-8), 7.45 (m, 1H, CH, H-6), 4.07 (m, 2H, 2 × CH, H-2‴, H-3‴), 3.94 (s, 3H, OCH_3), 3.81 (m, 2H, CH_2, H-1′), 2.95 (m, 2H, CH_2, H-4), 2.77 (m, 2H, CH_2, H-1), 2.49 (m, 6H, 3 × CH_2, H-2″, H-6″, H-10″), 1.97 (m, 3H, 3 × CH, H-3″, H-5″, H-8″), 1.82 (m, 6H, 3 × CH_2, H-2, H-3, H-2′), 1.58 (m, 6H, 3 × CH_2, H-4″, H-7″, H-9″); ^{13}C NMR (DMSO-d_6) δ 173.9 (C-1‴, C-4‴), 158.8 (C=O), 156.4 (C-7), 154.4 (C-9), 151.0 (C-4a), 134.2 (C-10a). 123.3 (C-6), 122.8 (C-5), 118.0 (C-9a), 111.9 (C-8a), 103.4 (C-8), 71.8 (C-2‴, C-3‴), 55.9 (OCH_3), 50.3 (C-1′), 42.1 (C-2′), 40.2 (C-2″, C-6″, C-10″), 36.2 (C-4″, C-7″, C-9″), 29.1 (C-4), 28.3 (C-3″, C-5″, C-8″), 24.9 (C-1), 22.2, 21.0 (C-2, C-3); Elemental analysis: calculated 62.19 % C, 7.07 % H, 9.36 % N; found 62.10 % C, 6.93 % H, 9.55 % N; ESI–MS: *m*/*z* 448.2 $[M]^+$ (calculated for: $[C_{27}H_{37}N_4O_2]^+$ 448.3).

*1-Adamantyl-3-(2-(7-methoxy-1,2,3,4-tetrahydroacridin-9-yl-amino)propyl)urea 2,3-dihydroxysuccinate (**12**)*

Yellow powder yields 90.1 %; m.p. = 75.2–78.1 °C; ^{1}H-NMR (DMSO-d_6) δ 7.81 (d, 1H, CH, H-5, J = 8.1 Hz), 7.66 (m, 1H, CH, H-8), 7.45 (d, 1H, CH, H-6), 4.11 (m, 2H, 2 × CH, H-2‴, H-3‴), 3.92 (s, 3H, OCH_3), 3.69 (m, 2H, CH_2, H-1′), 3.06 (m, 2H, CH_2, H-3′), 3.00 (m, 2H, CH_2, H-4), 2.74 (m, 2H, CH_2, H-1), 1.96 (m, 6H, 3 × CH_2, H-2″, H-6″, H-10″), 1.82 (m, 6H, 3 × CH_2, H-2, H-3, H-2′), 1.70 (m, 3H, 3 × CH, H-3″, H-5″, H-8″), 1.58 (m, 6H, 3 × CH_2, H-4″, H-7″, H-9″); ^{13}C NMR (DMSO-d_6) δ 174.0 (C-1‴, C-4‴), 158.1 (C=O), 156.5 (C-7), 154.1 (C-9), 151.0 (C-4a), 134.6 (C-10a), 123.4 (C-6), 122.8 (C-5), 118.2 (C-9a), 112.2 (C-8a), 103.0 (C-8), 72.0 (C-2‴,

C-3‴), 55.9 (OCH_3), 44.3 (C-1′), 42.1 (C-2′), 36.3 (C-4″, C-7″, C-9″), 35.6 (C-3′), 32.1 (C-3″, C-5″, C-8″), 29.1 (C-2″, C-6″, C-10″), 29.0 (C-4), 25.0 (C-1), 22.2, 20.9 (C-2, C-3); Elemental analysis: calculated 62.73 % C, 7.24 % H, 9.14 % N; found 62.32 % C, 7.20 % H, 9.05 % N; ESI–MS: *m/z* 462.2 $[M]^+$ (calculated for: $[C_{28}H_{39}N_4O_2]^+$ 462.3).

*1-Adamantyl-3-(2-(7-methoxy-1,2,3,4-tetrahydroacridin-9-yl-amino)butyl)urea 2,3-dihydroxysuccinate (**13**)*

White powder yields 67.0 %; m.p. = 80.5–83.3 °C; ^{1}H-NMR (DMSO-d_6) δ 7.79 (d, 1H, CH, H-5, J = 8.5 Hz), 7.59 (m, 1H, CH, H-8), 7.45 (m, 1H, CH, H-6), 4.03 (m, 2H, 2 × CH, H-2‴, H-3‴), 3.89 (s, 3H, OCH_3), 3.63 (m, 2H, CH_2, H-1′, 2.95 (m, 2H, CH_2, H-4), 2.93 (m, 2H, CH_2, H-4′), 2.70 (m, 2H, CH_2, H-1), 1.95 (m, 3H, 3 × CH, H-3″, H-5″, H-8″), 1.80 (m, 8H, 4 × CH_2, H-2, H-3, H-2′, H-3′), 1.57 (m, 6H, 3 × CH_2, H-2″, H-6″, H-10″), 1.37 (m, 6H, 3 × CH_2, H-4″, H-7″, H-9″); ^{13}C NMR (DMSO-d_6) δ 174.3 (C-1‴, C-4‴), 157.3 (C = O), 156.3 (C-7), 153.2 (C-9), 151.8 (C-4a), 136.2 (C-10a), 124.1 (C-6), 122.7 (C-5), 118.7 (C-9a), 113.3 (C-8a), 103.0 (C-8), 71.9 (C-2‴, C-3‴), 55.9 (OCH_3), 49.5 (C-1′), 47.0 (C-2′, C-3′), 38.6 (C-4′), 36.3 (C-4″, C-7″, C-9″), 29.8 (C-4), 29.1 (C-3″, C-5″, C-8″), 27.6 (C-2″, C-6″, C-10″), 25.0 (C-1), 22.3, 21.3 (C-2, C-3); Elemental analysis: calculated 63.24 % C, 7.40 % H, 8.94 % N; found 63.35 % C, 7.35 % H, 8.95 % N; ESI–MS: *m/z* 476.2 $[M]^+$ (calculated for: $[C_{29}H_{41}N_4O_2]^+$ 476.3).

*1-Adamantyl-3-(2-(7-methoxy-1,2,3,4-tetrahydroacridin-9-yl-amino)pentyl)urea 2,3-dihydroxysuccinate (**14**)*

White–yellow powder yield 87.9 %; m.p. = 83.8–86.2 °C; ^{1}H-NMR (DMSO-d_6) δ 7.79 (d, 1H, CH, H-5, J = 9.2 Hz), 7.60 (m, 1H, CH, H-8), 7.43 (dd, 1H, CH, H-6, J = 9.2, 2.1 Hz), 4.08 (m, 2H, 2 × CH, H-2‴, H-3‴), 3.89 (s, 3H, OCH_3), 3.67 (m, 2H, CH_2, H-1′), 2.96 (m, 2H, CH_2, H-4), 2.89 (m, 2H, CH_2, H-5′), 2.70 (m, 2H, CH_2, H-1), 1.95 (m, 3H, 3 × CH, H-3″, H-5″, H-8″), 1.80 (m, 8H, 4 × CH_2, H-2, H-3, H-3′ H-4′), 1.65 (m, 2H, CH_2, H-2′), 1.56 (m, 6H, 3 × CH_2, H-4″, H-7″, H-9″), 1.30 (m, 6H, 3 × CH_2, H-2″, H-6″, H-10″); ^{13}C NMR (DMSO-d_6) δ 174.0 (C-1‴, C-4‴), 157.3 (C=O), 156.4 (C-7), 153.8 (C-9), 151.3 (C-4a), 135.2 (C-10a), 123.3 (C-6), 123.1 (C-5), 118.3 (C-9a), 112.7 (C-8a), 103.3 (C-8), 71.9 (C-2‴, C-3‴), 56.0 (OCH_3), 47.2 (C-1′), 42.2 (C-3′, C-4′), 38.8 (C-5′), 36.3 (C-4″, C-7″, C-9″), 30.3 (C-2′), 29.3 (C-4), 29.1 (C-3″, C-5″, C-8″), 24.9 (C-1), 23.8 (C-2″, C-6″, C-10″), 22.1, 21.0 (C-2, C-3); Elemental analysis: calculated 63.73 % C, 7.55 % H, 8.74 % N; found 63.60 % C, 7.60 % H, 8.55 % N; ESI–MS: *m/z* 490.2 $[M]^+$ (calculated for: $[C_{30}H_{43}N_4O_2]^+$ 490.3).

*1-Adamantyl-3-(2-(7-methoxy-1,2,3,4-tetrahydroacridin-9-yl-amino)hexyl)urea 2,3-dihydroxysuccinate (**15**)*

Yellow powder yields 67.0 %; m.p. = 84.0–86.8 °C; ^{1}H-NMR (DMSO-d_6) δ 7.80 (d, 1H, CH, H-5, J = 9.1 Hz), 7.60 (m, 1H, CH, H-8), 7.42 (dd, 1H, CH, H-6, J = 9.1, 2.2 Hz), 4.07 (m, 2H, 2 × CH, H-2‴, H-3‴), 3.89 (s, 3H, OCH_3), 3.66 (t, 2H, CH_2, H-1′, J = 6.1 Hz), 2.96 (m, 2H, CH_2, H-4), 2.87 (m, 2H, CH_2, H-6′), 2.70 (m, 2H, CH_2, H-1), 1.95 (m, 3H, 3 × CH, H-3″, H-5″ H-8″), 1.81 (m, 8H, 4 × CH_2, H-2, H-3, H-4′, H-5′), 1.63 (m, 2H, CH_2, H-2′), 1.56 (m, 6H, 3 × CH_2, H-4″, H-7″, H-9″), 1.31 (m, 8H, 4 × CH_2, H-3′, H-2″, H-6″, H-10″); ^{13}C NMR (DMSO-d_6) δ 174.0 (C-1‴, C-4‴), 157.3 (C=O), 156.4 (C-7), 153.7 (C-9), 151.4 (C-4a), 135.4 (C-10a), 123.5 (C-6), 123.0 (C-5), 118.4 (C-9a), 112.8 (C-8a), 103.2 (C-8), 71.9 (C-2‴, C-3‴), 55.9 (OCH_3), 47.0 (C-1′), 42.2 (C-4′, C-5′), 38.7 (C-6′), 36.3 (C-4″, C-7″, C-9″), 30.6 (C-2′), 30.2 (C-3′), 29.4 (C-4), 29.1 (C-3″, C-5″, C-8″), 26.1 (C-2″, C-6″, C-10″), 25.0 (C-1), 22.2, 21.1 (C-2, C-3); Elemental analysis: calculated 64.20 % C, 7.70 % H, 8.56 % N; found 64.15 % C, 7.83 % H, 8.50 % N; ESI–MS: *m/z* 504.3 $[M]^+$ (calculated for: $[C_{31}H_{45}N_4O_2]^+$ 504.4).

*1-Adamantyl-3-(2-(7-methoxy-1,2,3,4-tetrahydroacridin-9-yl-amino)heptyl)urea 2,3-dihydroxysuccinate (**16**)*

Orange powder yields 81.5 %; m.p. = 65.2–68.2 °C; ^{1}H-NMR (DMSO-d_6) δ 7.80 (d, 1H, CH, H-5, J = 9.1 Hz), 7.62 (m, 1H, CH, H-8), 7.44 (m, 1H, CH, H-6), 4.10 (m, 2H, 2 × CH, H-2‴, H-3‴), 3.89 (s, 3H, OCH_3), 3.68 (t, 2H, CH_2, H-1′, J = 6.5 Hz), 2.96 (m, 2H, CH_2, H-4), 2.86 (m, 2H, CH_2, H-7′), 2.69 (m, 2H, CH_2, H-1), 1.95 (m, 3H, 3 × CH, H-3″, H-5″, H-8″), 1.81 (m, 8H, 4 × CH_2, H-2, H-3, H-5′ H-6′, 1.65 (m, 2H, CH_2, H-2′, 1.56 (m, 6H, 3 × CH_2, H-4″, H-7″, H-9″), 1.23 (m, 8H, 4 × CH_2, H-3′, H-2″, H-6″, H-10″); ^{13}C NMR (DMSO-d_6) δ 173.9 (C-1‴, C-4‴), 157.3 (C=O), 156.4 (C-7), 153.9 (C-9), 151.1 (C-4a), 135.0 (C-10a), 123.2 (C-6), 123.1 (C-5), 118.2 (C-9a), 112.6 (C-8a), 103.3 (C-8), 72.0 (C-2‴, C-3‴), 56.0 (OCH_3), 47.1 (C-1′), 42.2 (C-5′, C-6′), 38.9 (C-7′), 36.3 (C-4″, C-7″, C-9″), 30.5 (C-2′), 30.1 (C-3′), 29.4 (C-4), 29.1 (C-3″, C-5″, C-8″), 28.6 (C-4′), 26.4 (C-2″, C-6″, C-10″), 24.9 (C-1), 22.1, 21.0 (C-2, C-3); Elemental analysis: calculated 64.65 % C, 7.84 % H, 8.38 % N; found 64.58 % C, 7.83 % H, 8.40 % N; ESI–MS: *m/z* 518.4 $[M]^+$ (calculated for: $[C_{32}H_{47}N_4O_2]^+$ 518.5).

*1-Adamantyl-3-(2-(7-methoxy-1,2,3,4-tetrahydroacridin-9-yl-amino)octyl)urea 2,3-dihydroxysuccinate (**17**)*

Yellow–brown powder yield 60.1 %; m.p. = 57.3–60.0 °C; ^{1}H-NMR (DMSO-d_6) δ 7.81 (d, 1H, CH, H-5, J = 9.1 Hz),

7.61 (m, 1H, CH, H-8), 7.44 (m, 1H, CH, H-6), 4.10 (m, 2H, 2 × CH, H-2‴, H-3‴), 3.89 (s, 3H, OCH_3), 3.68 (t, 2H, CH_2, H-1′ $J = 6.8$ Hz), 2.96 (m, 2H, CH_2, H-4), 2.86 (m, 2H, CH_2, H-8′), 2.69 (m, 2H, CH_2, H-1), 1.95 (m, 3H, 3 × CH, H-3″, H-5″, H-8″), 1.81 (m, 8H, 4 × CH_2, H-2, H-3, H-6′, H-7′), 1.65 (m, 2H, CH_2, H-2′), 1.56 (m, 6H, 3 × CH_2, H-4″, H-7″, H-9″), 1.23 (m, 10H, 5 × CH_2, H-3′, H-4′, H-2″, H-6″, H-10″); ^{13}C NMR (DMSO-d_6) δ 174.0 (C-1‴, C-4‴), 157.3 (C=O), 156.4 (C-7), 153.9 (C-9), 151.2 (C-4a), 135.0 (C-10a), 123.2 (C-6), 123.1 (C-5), 118.2 (C-9a), 112.6 (C-8a), 103.3 (C-8), 72.0 (C-2‴, C-3‴), 56.0 (OCH_3), 47.1 (C-1′), 42.2 (C-6′, C-7′), 38.9 (C-8′), 36.3 (C-4″, C-7″, C-9″), 30.5 (C-2′), 30.2 (C-3′), 29.4 (C-4), 29.1 (C-3″, C-5″, C-8″), 28.8 (C-4′), 26.4 (C-2″, C-6″, C-10″), 24.9 (C-1), 22.1, 21.0 (C-2, C-3); Elemental analysis: calculated 65.08 % C, 7.97 % H, 8.20 % N; found 65.01 % C, 8.10 % H, 8.35 % N; ESI–MS: *m/z* 532.4 $[M]^+$ (calculated for: $[C_{33}H_{49}N_4O_2]^+$ 532.5).

In vitro testing

A sunrise multichannel spectrophotometer (Tecan, Salzburg, Austria) was used for all cholinesterase activity measurements. A previously optimized Ellman procedure was slightly modified in order to estimate anticholinergic properties (Bielavsky, 1977). 96-well photometric microplates made from polystyrene (Nunc, Rockilde, Denmark) were used for measuring purposes. Human recombinant AChE or human plasmatic BChE (Aldrich; commercially purified by affinity chromatography) was suspended into phosphate buffer (pH 7.4) up to final activity 0.002 U/μL. Cholinesterase (5 μL), freshly mixed solution of 0.4 mg/mL 5,5′-dithio-bis(2-nitrobenzoic) acid (40 μL), 1 mM acetylthiocholine chloride in phosphate buffer (20 μL) and appropriate concentration of inhibitor (1 mM–0.1 nM; 5 μL), were injected per well. Absorbance was measured at 412 nm after 5-min incubation using automatic shaking of the microplate. The obtained data were used to compute percentage of inhibition (I; Eq. 1):

$$I = 1 - \frac{\Delta A_i}{\Delta A_0}[\%] \quad (1)$$

where ΔA_i indicates absorbance change provided by cholinesterase exposed to *h*AChE inhibitors, and ΔA_0 indicates absorbance change caused by intact cholinesterase (phosphate buffer was applied instead of *h*AChE inhibitor). IC_{50} values were calculated using Origin 6.1 (Northampton, MA, USA). Percentage of inhibition for the given anticholinergic compound was overlaid by proper curve chosen according to optimal correlation coefficient. IC_{50} as well as upper limit of inhibition (maximal inhibition provided by given compound) was computed.

Molecular modelling studies

Docking calculations were performed using AutoDock Vina (Yan and Wang, 2012). The molecular models were built and minimized with UCSF chimera 1.3 (Amber Force Filed) (Trott and Olson, 2010). The structure of both enzymes, human AChE (*h*AChE, PDB ID: 1B41) and human BChE (*h*BChE, PDB ID: 1P0I), was prepared using PyMol 1.1 from crystal structures (Pettersen *et al.*, 2004; Kryger *et al.*, 2000). Compounds used in this study and both enzymes were prepared using AutoDock Tools 1.5.2. in charged form (The Pymol Molecular Graphics System, Morris *et al.*, 2009). Molecules of water with other non-enzymatic molecules were removed (withdrawing the fasciculin 2 from *h*AChE and molecules of water from both enzymes), and hydrogens were added (Harel *et al.*, 1993). The 3D affinity grid box in the *x*-, *y*- and *z*-axes was 66, 66 and 66 with spacing 0.253 Å for *h*AChE, within the *h*BChE grid box dimensions were set to $x = 46$, $y = 60$ and $z = 46$ with spacing 0.375 Å. For the *h*AChE docking, the grid for energy was set in the coordinates $x = 119.775$, $y = 117.597$ and $z = -128.964$, within *h*BChE the coordinates were adjusted to $x = 137.871$, $y = 115.156$ and $z = 38.652$. The *h*AChE residues Trp86, Tyr72, Trp286, Asp74, Tyr341 and Phe297 were set to be flexible by AutoDock Tools 1.5.2, for *h*BChE amino acid residues Glu325, His438, Trp82, Asp70 and Tyr332 were selected as flexible. Flexible ligand docking was performed for the selected compound **14** and compared to previously reported compound **7**. The docking calculations were made on Mac Pro 4.1 Quad-Core Intel Xeon 2.93 GHz. At the end of calculation, AutoDock Vina performed cluster analysis. The visualization was carried out in PyMol 1.1. Hydrogens were finally removed to improve figures clarity.

Results and discussion

Chemistry

The synthesis of prepared 7-MEOTA-amantadine thioureas 2,3-dihydroxysuccinates **4–10** was described in previous work (Spilovska *et al.*, 2013). The preparation of 1-adamantyl-3-(2-(7-methoxy-1,2,3,4-tetrahydroacridin-9-yl-amino)octyl)ureas 2,3-dihydroxysuccinates **11–17** was accomplished in two steps. The 7-MEOTA-amantadine thioureas were transferred to 7-MEOTA-amantadine ureas using 2,4,6-trimethylbenzonitril-*N*-oxide (MNO) as oxidative agent. The reaction was performed in dichloromethane for 24 h at room temperature. The formation of urea moiety was confirmed by the ^{13}C NMR signal in the range 156–159 ppm for the carbonyl carbon. The final heterodimers were converted to tartaric salts by addition

Scheme 1 Synthesis of 7-MEOTA-amantadine ureas derivatives

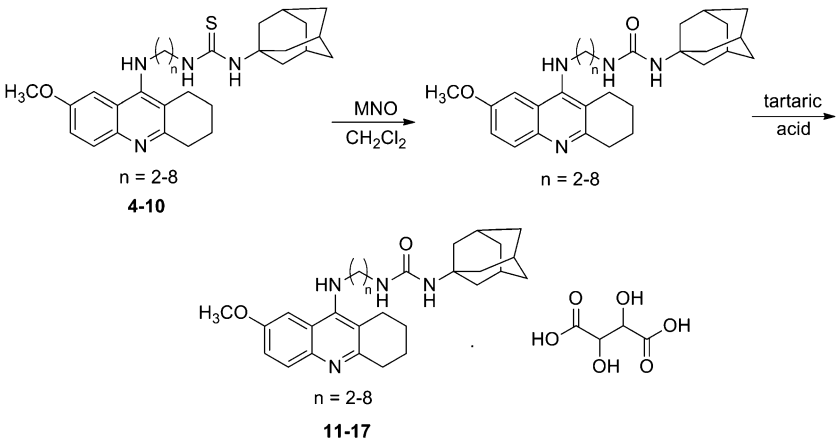

of equimolar amount of tartaric acid. The conversion to tartaric salt was necessary for better solubility for in vitro assessment. 7-MEOTA-amantadine ureas 2,3-dihydroxysuccinates were acquired in yields ranging from 60 to 90 %. The synthetic route leading to novel heterodimers **11–17** is shown in Scheme 1.

Biological assay

The AChE and BChE inhibitory activity of all 14 7-MEOTA-amantadine derivatives were determined by the spectroscopic method described by Ellman *et al.* using human AChE and BChE (Ellman *et al.*, 1961; Pohanka *et al.*, 2008). Amantadine, THA and 7-MEOTA were used as standards. The results were expressed as IC_{50} values for *h*AChE/*h*BChE, and they are summarized in Table 1. The novel urea heterodimers seem to have a favourable effect on AChE and BChE inhibition. Compared to THA, which had IC_{50} 0.5 μM for *h*AChE and IC_{50} 0.023 μM for *h*BChE, the other two reference standards (7-MEOTA and amantadine) were less potent inhibitors.

7-MEOTA and amantadine exhibited two orders of magnitude decrease in *h*AChE inhibitory activity in comparison with THA. Moreover, THA was stronger *h*BChE inhibitor compared to 7-MEOTA and amantadine. All new hybrids were more potent *h*AChE and *h*BChE inhibitors than 7-MEOTA with IC_{50} values ranging from 5.02 to 0.47 μM for thioureas (**4–10**) and from 4.98 to 0.69 μM for ureas (**11–17**). In the 7-MEOTA-amantadine thioureas, series five compounds had IC_{50} values in sub-micromolar range for *h*AChE. Only two derivatives (**5** and **7**) exhibited inhibition potency in sub-micromolar range for *h*AChE. However, compounds **4, 7, 8, 9** and **10** showed sub-micromolar inhibition potency for *h*BChE. The best inhibitory activity from **4** to **10** had compound **7**, bearing five methylene groups in the linker. This derivative displayed potency in the same order of magnitude to THA for *h*AChE. The selectivity index (SI) was calculated for all newly evaluated compounds. All novel compounds (except analogues **5**, **12** and **17**) have lower SI values compared to 7-MEOTA or amantadine and can be considered as agents more selective for *h*BChE.

The 7-MEOTA-amantadine ureas series **11–17** were synthesized and biologically evaluated to determine different binding affinities towards both human cholinesterases. These heterodimers demonstrated potent inhibitory activity against *h*AChE and *h*BChE with IC_{50} values ranging from the micromolar to sub-micromolar. In particular, compound **14** represented by 7-MEOTA and amantadine linked with five carbon chain exhibited the highest inhibition activity of *h*AChE and *h*BChE. However, this derivative resulted in a 1.4-fold decreased activity for *h*AChE and 9.6-fold decreased inhibition potency for *h*BChE relative to THA. Furthermore, compound **14** was ascertained to be 15.2-fold more potent inhibitor of *h*AChE than 7-MEOTA. None of the novel compounds presented significant activity in comparison with nanomolar galantamine-memantine dimers (**1–3**, Table 1).

Considering differences between 7-MEOTA-amantadine thioureas and their urea analogues in relation to the linker length, thioureas derivatives **4–7** and **10** had very similar IC_{50} values as their urea analogues **11–14** and **17** for *h*AChE. By other two thiourea (**8**, **9**) and urea derivatives (**15**, **16**), this trend in inhibition ability was not observed. Essentially, compound **8** and **9** exhibited one order of magnitude higher inhibitory activity than heterodimers **15** and **16**. Moreover, five derivatives of urea (**11**, **12**, **13**, **15**, **16**) proved enhanced inhibitory capability for *h*AChE in comparison with their thiourea counterparts. Regarding the inhibitory activity of tested ureas for *h*BChE (apart from the analogue **14**), these hybrids had lower inhibition ability than original thioureas. However, the difference in the IC_{50} values was statistically insignificant. Regarding selectivity index results, 7-MEOTA was found more selective towards

Table 1 IC_{50} values of reference standards and tested heterodimers and log*P* values

Compound	IC_{50} (μM) ± SD[a] (*h*AChE)	IC_{50} (μM) ± SD (*h*BChE)	SI[b]	log*P*[d]
1	0.00116 ± 0.00003[c]	–	–	6.53 ± 0.81
2	0.00179 ± 0.00006	–	–	7.06 ± 0.81
3	0.0113 ± 0.0016	–	–	5.38 ± 0.84
4	5.02 ± 0.98	6.02 ± 1.01	1.2	6.54 ± 0.80
5	0.53 ± 0.10	1.39 ± 0.23	2.6	7.73 ± 1.04
6	2.04 ± 0.39	0.98 ± 0.16	0.5	8.12 ± 1.04
7	0.47 ± 0.09	0.11 ± 0.02	0.2	7.59 ± 0.79
8	2.09 ± 0.40	0.33 ± 0.05	0.2	8.12 ± 0.79
9	3.47 ± 0.67	0.15 ± 0.02	0.04	8.66 ± 0.79
10	1.62 ± 0.31	0.26 ± 0.04	0.2	9.19 ± 0.79
11	4.98 ± 0.97	2.82 ± 0.47	0.6	5.87 ± 0.83
12	0.52 ± 0.10	2.18 ± 0.36	4.2	6.20 ± 0.83
13	1.94 ± 0.38	1.79 ± 0.30	0.9	6.58 ± 0.83
14	0.69 ± 0.13	0.22 ± 0.04	0.3	6.92 ± 0.83
15	0.85 ± 0.17	1.01 ± 0.17	1.2	7.45 ± 0.83
16	0.69 ± 0.14	0.44 ± 0.07	0.6	7.99 ± 0.83
17	2.03 ± 0.40	18.82 ± 3.14	9.3	8.52 ± 0.83
THA	0.50 ± 0.10	0.023 ± 0.003	0.05	3.32 ± 0.25
7-MEOTA	10.50 ± 2.40	21.00 ± 3.40	2.0	3.41 ± 0.74
Amantadine	16.05 ± 3.13	102.60 ± 17.13	6.4	2.22 ± 0.24

[a] The in vitro concentration of tested compound required to produce 50 % inhibition of *h*AChE/*h*BChE. Results are the mean of three independent measurements ± standard deviation

[b] Selectivity index (SI) for *h*AChE is determined as ratio of IC_{50} *h*BChE towards IC_{50} *h*AChE

[c] Data for compounds **1**–**3**, determined using rat AChE, are taken from the reference. Simoni *et al.* (2012)

[d] Predicted data were generated using ACD/labs system

*h*AChE, whereas heterodimers **7** and **14** were predominantly selective towards *h*BChE. As shown in Table 1, from both series of thiourea and urea, derivatives are the best cholinesterase inhibitors compounds **7** and **14** bearing five methylene groups in the linker. This may be due the fact that so long linker is optimal to interact with the gorge of the enzyme in comparison with other thiourea and urea heterodimers. Futhermore, IC_{50} values of these two inhibitors **7** and **14** are very similar. Enzyme activities for reference standards THA and 7-MEOTA and of tested urea **14** for *h*AChE/*h*BChE are displayed in Figs. 2 and 3.

Based on the fact that studying lipophilicity is important in the evaluation of anti-AD drugs, the log*P* values were calculated. The log*P* (partition coefficient) is one of the important coefficients, which was well-defined by Lipinski in the "rule of five" for "drug-like" molecules (Lipinski *et al.*, 2001). According to Lipinski, log*P* value for chemical compounds to be centrally active should be less than five. The log*P* values for 7-MEOTA-amantadine thiourea and urea derivatives are displayed in Table 1. All of the compounds showed log*P* values more than five proposing their highly lipophilic character. In comparison with thiourea subset, urea derivatives demonstrated lower log*P* values,

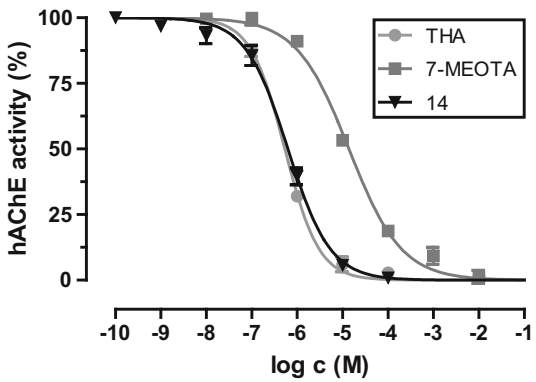

Fig. 2 *h*AChE activity for THA, 7-MEOTA and **14**

plausibly due to their ability to easier formation of hydrogen bonds with amino acid residues within ChE active site. Even though newly synthesized inhibitors possess log*P* values far from the optimal, their effect to cross-biological membranes needs to be determined in vivo.

Based on in vitro results, it is not clear whether the most active urea analogue manages higher potency towards both binding sites (active and peripheral) of *h*AChE as thiourea

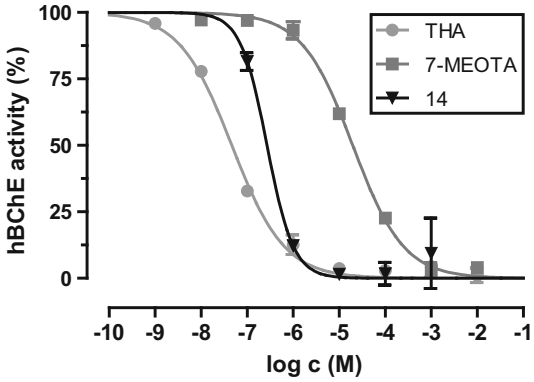

Fig. 3 *h*BChE activity for THA, 7-MEOTA and **14**

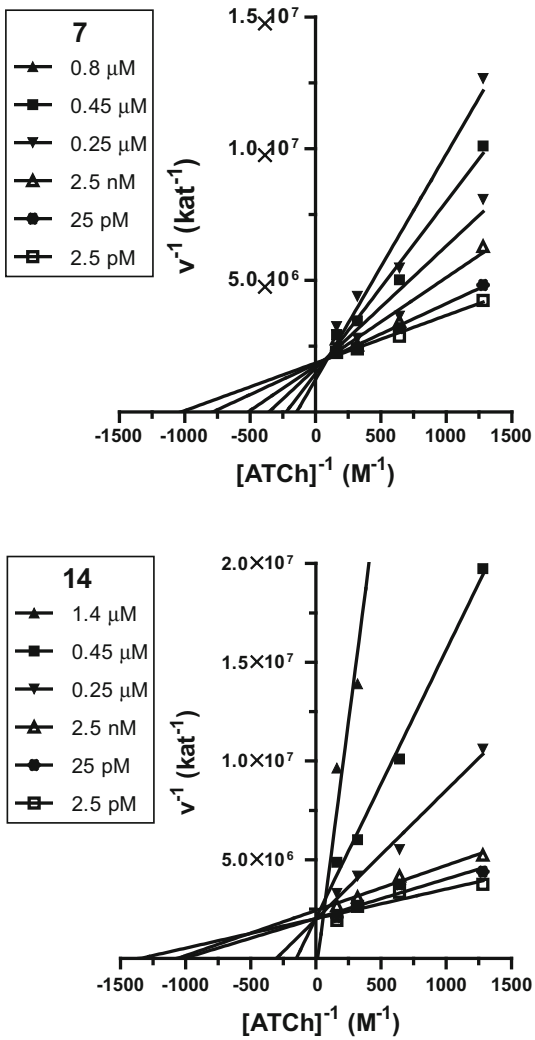

Fig. 4 Steady-state inhibition of *h*AChE hydrolysis substrate ATCh by compounds **7** and **14**. Lineweaver–Burk reciprocal plots of initial velocity and substrate concentrations (0.781–6.25 nM) for different concentrations of tested inhibitors. *Lines* were derived from a weighted least-squares analysis of data

analogue with the same spacer length. Therefore, only the most promising inhibitors (**7** and **14**) were subjected to kinetic analysis of the *h*AChE inhibition and molecular modelling studies to clarify the differences in their binding.

The inhibition mechanism of compounds **7** and **14** was investigated using steady-state inhibition of acetylthiocholine (ATCh) hydrolysis. The inhibition type was elucidated from the nonlinear regression analysis using GraphPad Prism 5.02 software (GraphPad Software, San Diego, CA, USA). Results for each inhibition model (competitive, noncompetitive, uncompetitive and mixed) were compared with sum of squares *F* test. Analysis confirmed competitive type of inhibition ($p < 0.05$) for both compounds. Figure 4 shows Lineweaver–Burk reciprocal plots of measured data. A K_i value 0.409 ± 0.157 μM for inhibitor **7** and 0.163 ± 0.057 μM for **14** was estimated by the nonlinear regression analysis.

Molecular docking simulations for derivative **14** into *h*AChE active site were performed using the AutoDock Tools 1.5.2 software. We used the X-ray structure of the *h*AChE-fasciculin-2 complex (PDB ID: 1B41), as the enzyme of same origin was used in the in vitro biochemical assay (Fig. 5). Moreover, *h*AChE obtained from PDB is available in high resolution and represents a good tool for molecular modeling. Acquired docking simulations showed dual binding site character; 7-MEOTA moiety was observed to enter the catalytic anionic site (CAS), while adamantyl cage is located at the peripheral anionic site (PAS) (Fig. 5). 7-MEOTA moiety provides parallel π–π stacking with Trp86 (3.4 Å) and cation-π contact with Tyr337 (3.4 Å). Tyr337 could provide additional hydrogen bonding between the heterocyclic tacrine

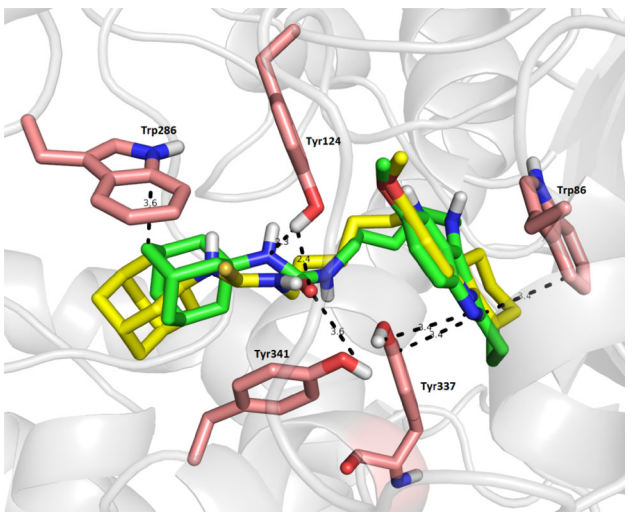

Fig. 5 Top-scored docking poses of the compounds **14**- and **7**-*h*AChE complex. The binding pattern of compound **14** is shown in *green*, previously reported analogue **7** is depicted in *yellow* and important amino acid residues are highlighted in *pale-brown* (Color figure online)

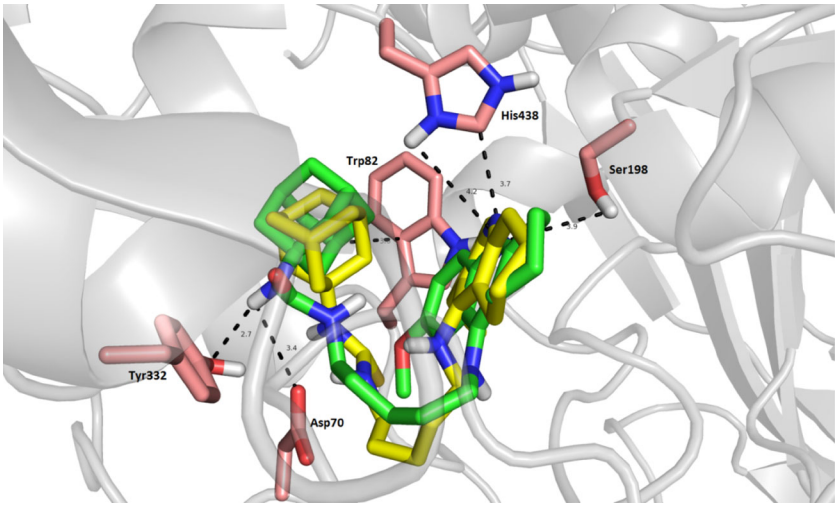

Fig. 6 Two major binding modes of **14** (*green*) and **7** (*yellow*) *h*BChE. Both compounds as well as attached amino acid residues (*pale-brown*) are rendered as *sticks* (Color figure online)

nitrogen and the Tyr337 hydroxyl group. Adamantyl scaffold could have aliphatic-π contact with both Trp286 (3.6 Å), and Phe297 (4.0 Å) and several weak Van der Waals interactions (Val294—4.1 Å, Leu289—4.1 Å). Spacer has two sections: urea group interacts via hydrogen bonds to Tyr124 (2.3 Å, 2.4 Å) and Tyr341 (3.6 Å), while methylene bridge is constricted to aromatic amino acid residues (Phe338—3.6 Å; Phe297—3.7 Å) through hydrophobic interactions. The binding energy for **14** (−12.0 kcal/mol) is similar to that found for the most potent derivative **7** (−11.1 kcal/mol) in the 7-MEOTA-amantadine thiourea class. Similar spatial orientation of **7** and **14** within *h*AChE active site can explain similar in vitro activity (Table 1). Only His438 (3.9 Å), from the catalytic triad seems to provide weak hydrophobic interaction with cyclohexyl moiety of 7-MEOTA.

The flexible docking procedure was applied to *h*BChE (PDB ID: 1P01) to determine possible differences of binding modes concerning compounds **14** and **7**. Since no crystal structure of tacrine and tacrine derivatives within *h*BChE active site is available the choice of *h*BChE crystal structure from PDB was based on a good resolution of the enzyme. In addition, the enzyme of the same origin was used in the in vitro assay. The docking simulations confirmed predicted orientations for both derivatives **14** (−10.4 kcal/mol) and **7** (−10.3 kcal/mol) with minor changes in their spatial arrangements (Fig. 6). Evaluation of **14** revealed hydrogen bond interactions between heterocyclic nitrogen of 7-MEOTA moiety and amino acid residues of catalytic triad, Ser198 (3.9 Å), His438 (4.2 Å), while Glu325 is not affected. His438 (3.7 Å) also provides T-shaped π–π interaction. Besides the three ring core of **14,** it is also involved in T-shaped π–π interaction with Phe329 (4.3 Å) and parallel π–π stacking with Trp231 (4.0 Å). Furthermore, the most energetically favoured binding mode of **14** places the adamantyl skeleton to vicinity of Trp82 (3.6 Å), Tyr440 (4.1 Å) and Trp440 (4.9 Å) displaying aliphatic-π contact. In this orientation, urea moiety in the linker established hydrogen bonding to Tyr332 (2.7 Å) and Asp70 (3.4 Å).

Conclusion

In conclusion, we have reported the synthesis and pharmacological evaluation of a new series of multi-target-directed ligands derived from 7-MEOTA and amantadine for the treatment of AD. Our study extended the previously reported series of biologically active 7-MEOTA-amantadine thiourea derivatives to 7-MEOTA-amantadine ureas. These urea analogues were evaluated as potential inhibitors of AChE and BChE, but expected rise in cholinesterase inhibition potency was not observed. The Lineweaver–Burk plot revealed that the best thiourea derivate **7** and best urea analogue **14** inhibited *h*AChE competitively. Further investigations of AD therapeutic candidates (anti-amyloid aggregation, channel activity of NMDA receptor) based on these results are in progress.

Acknowledgments This study was supported by the specific research (SV/FVZ201201), by the Grant Agency of the Czech Republic (No. P303/11/1907), FIM excellence project, by Post-doctoral project (No. CZ.1.07/2.3.00/30.0044), by MH CZ-DRO (University Hospital Hradec Kralove, No. 00179906), by Long Term Development plan – 1011, by Vega 0181, APVV 0171-10, and by project 26220220005 in the framework of the Structural Funds of European Union.

References

Bartolini M, Bertuci C, Bolognesi ML, Cavalli A, Melchiorre C, Andrisano V (2007) Insight into the kinetic of amyloid beta (1–42) peptide self-aggregation: elucidation of inhibitors' mechanism of action. ChemBioChem 8(17):2152–2161

Bielavsky J (1977) Analogues of 9-amino-1,2,3,4-tetrahydroacridine. Collect Czechoslov Chem Commun 42(9):2802–2808

Blanpied TA, Clarke RJ, Johnson JW (2005) Amantadine inhibits NMDA receptors by accelerating channel closure during channel block. J Neurosci 25(13):3312–3322

Bormann J (1989) Memantine is a potent blocker of *N*-methyl-D-aspartate (NMDA) receptor channels. Eur J Pharmacol 166(3):591–592

Caumont AS, Octave JN (2006) Amantadine and memantine induce the expression of the glial cell line-derived neurotrophic factor in C6 glioma cells. Neurosci Lett 394(3):196–201

Cavalli A, Bolognesi ML, Minarini A, Rosini M, Tumiatti V, Recanatini M, Melchiorre C (2008) Multi-target- directed ligands to combat neurodegenerative diseases. J Med Chem 51(3):347–372

Craig LA, Hong NS, McDonald RJ (2011) Revisiting the cholinergic hypothesis in the development of Alzheimer's disease. Neurosci Biobehav Rev 35(6):1397–1409

Cummings JL (2004) Treatment of Alzheimer's disease: current and future therapeutic approaches. Rev Neurol Dis 1(2):60–69

Darvesh S, Hopkins DA, Geula C (2003) Neurobiology of butyrylcholinesterase. Nat Rev Neurosci 4(2):131–138

Dejmek L (1990) 7-MEOTA. Drugs Future 15:126–129

Ellman GL, Courtney KD, Andres V, Feather-Stone RM (1961) A new and rapid colorimetric determination of acetylcholinesterase activity. Biochem Pharmacol 7:88–95

Forest Pharmaceuticals Inc (2003) Namenda package insert. Forest Pharmaceuticals Inc., St. Louis

Gauthier S, Poirier J (2008) Current and future management of Alzheimer's disease. Alzheimers Dement 4(1 Suppl 1):S48–S50

Giacobini E (2004) Cholinesterase inhibitors: new roles and therapeutic alternatives. Pharmacol Res 50(4):433–440

Greig NH, Utsuki T, Yu QS, Zhu X, Holloway HW, Perry T, Lee B, Ingram DK, Lahiri DK (2001) A new therapeutic target in Alzheimer's disease treatment: attention to butyrylcholinesterase. Curr Med Res Opin 17(3):159–165

Greig NH, Utsuki T, Ingram DK, Wang Y, Pepeu G, Scali C, Yu QS, Mamczarz J, Holloway HW, Giordano T, Chen D, Furukawa K, Sambamurti K, Brossi A, Lahiri DK (2005) Selective butyrylcholinesterase inhibition elevates brain acetylcholine, augments learning and lower Alzheimer beta-amyloid peptide in rodent. Proc Natl Acad Sci USA 102(47):17213–17218

Harel M, Schalk I, Ehret-Sabatier L, Bouet F, Goeldner M, Hirth C, Axelsen PH, Silman I, Sussman JL (1993) Quaternary ligand binding to aromatic residues in the active-site gorge of acetylcholinesterase. Proc Natl Acad Sci USA 90(19):9031–9035

Jahn H (2013) Memory loss in Alzheimer's disease. Dialogues Clin Neurosci 15(4):445–454

Korabecny J, Musilek K, Holas O, Binder J, Zemek F, Pohanka M, Opletalova V, Dohnal V, Kuca K (2010) Synthesis and in vitro evaluation of N-alkyl-7-methoxytacrine hydrochlorides as potential cholinesterase inhibitors in Alzheimer's disease. Bioorg Med Chem Lett 20(20):6093–6095

Korabecny J, Musilek K, Zemek F, Horova A, Holas O, Nepovimova E, Opletalova V, Hroudova J, Fisar Z, Jung YS, Kuca K (2011) Synthesis and in vitro evaluation of 7-methoxy-N-(pent-4-enyl)-1,2,3,4-tetrahydroacridin-9-amine—new tacrine derivate with cholinergic properties. Bioorg Med Chem Lett 21(21):6563–6566

Korabecny J, Dolezal R, Cabelova P, Horova A, Hruba E, Ricny J, Sedlacek L, Nepovimova E, Spilovska K, Andrs M, Musilek K, Opletalova V, Sepsova V, Ripova D, Kuca K (2014) 7-MEOTA-donepezil like compounds as cholinesterase inhibitors: synthesis, pharmacological evaluation, molecular modeling and QSAR studies. Eur J Med Chem 82:426–438

Kotermanski SE, Johnson JW (2009) Mg2 + imparts NMDA receptor subtype selectivity to the Alzheimer's drug memantine. J Neurosci 29(9):2774–2779

Krall WJ, Sramek JJ (1999) Cholinesterase inhibitors: a therapeutic strategy for Alzheimer disease. Ann Pharmacother 33(4):441–450

Kryger G, Harel M, Giles K, Toker L, Velan B, Lazar A, Kronman C, Barak D, Ariel N, Shafferman A, Silman I, Sussman JL (2000) Structures of recombinant native and E202Q mutant human acetylcholinesterase complexed with the snake-venom toxin fasciculin-II. Acta Crystallogr D Biol Crystalogr 56(Pt 11):1385–1394

Lahiri DK, Farlow MR, Sambamurti K, Greig NH, Giacobini E, Schneider LS (2003) A critical analysis of new molecular targets and strategies for drug developments in Alzheimer's disease. Curr Drug Targets 4(2):97–112

Lipinski CA, Lombardo FM, Dominy BW, Feeney PJ (2001) Experimental and computational approaches to estimate solubility and permeability in drug discovery and development settings. Drug Deliv Rev 46(1–3):3–26

Lipton SA (2006) Paradigm shift in neuroprotection by NMDA receptor blockade: memantine and beyond. Nat Rev Drug Discov 5(2):160–170

Magazanik LG, Antonov SM, Lukomskaya NY, Potapeva NN, Gmiro VE, Johnson J (1996) Blockade of glutamate- and cholinergic ion channels by amantadane derivatives. Neurosci Behav Physiol 26(1):13–22

Manning SM, Boll G, Fitzgerald E, Selip DB, Volpe JJ, Jensen FE (2011) The clinically available NMDA receptor antagonist, memantine, exhibits relative safety in the developing rat brain. Int J Dev Neurosci 29(7):767–773

Marx JL (1987) Alzheimer's drug trial put on hold. Science 238(4830):1041–1042

Mayeux R (2003) Epidemiology of neurodegeneration. Annu Rev Neurosci 26:81–104

Morris GM, Huey R, Lindstrom W, Sanner MF, Belew RK, Goodsell DS, Olson AJ (2009) AutoDock4 and AutoDock Tools4: automated docking with selective receptor flexibility. J Comput Chem 30(16):2785–2791

Ossola B, Schendzielorz N, Chen SH, Bird GS, Tuominen RK, Mannisto PT, Hong JS (2011) Amantadine protects dopamine neurons by a dual action: reducing activation microglia and inducing expression of GDNF in astroglia. Neuropharmacology 61(4):574–582

Page G, Peeters M, Maloteaux JM, Hermans E (2000) Increased dopamine uptake in striatal synaptosomes after treatment of rats with amantadine. Eur J Pharmacol 403(1–2):75–80

Patocka J, Jun D, Kuca K (2008) Possible role of hydroxylated metabolites of tacrine in drug toxicity and therapy of Alzheimer's disease. Curr Drug Metab 9(4):332–335

Peeters M, Page G, Maloteaux JM, Hermans E (2002) Hypersensitivity of dopamine transmission in the rat striatum after treatment with the NMDA receptor antagonist amantadine. Brain Res 949(1–2):32–41

Pettersen EF, Goddard TD, Huang CC, Couch GS, Greenblatt DM, Meng EC, Ferrin TE (2004) UCSF Chimera—a visualization system for exploratory research and analysis. J Comput Chem 25(13):1605–1612

Pohanka M, Jun D, Kuca K (2008) Improvement of acetylcholinesterase-based assay for organophosphates in was of identification by reactivators. Talanta 77(1):451–454

Rizzo S, Bisi A, Bartolini M, Mancini F, Belluti F, Gobbi S, Andrisano V, Rampa A (2011) Multi-target strategy to address Alzheimer's disease: design, synthesis and biological evaluation of new tacrine-based dimers. Eur J Med Chem 46(9):4336–4343

Schmitt HP (2005) On the paradox of ion channel blockade and its benefits in the treatment of Alzheimer disease. Med Hypotheses 65(2):259–265

Silman I, Sussman JL (2005) Acetylcholinesterase: "classical" and "non-classical" functions and pharmacology. Curr Opin Pharmacol 5(3):293–302

Simoni E, Daniele S, Bottegoni G, Pizzirani D, Trincavelli ML, Goldoni L, Tarozzo G, Reggiani A, Martini C, Piomelli D, Melchiorre C, Rosini M, Cavalli A (2012) Combining galantamine and memantine in multitargeted, new chemical entities potentially useful in Alzheimer's disease. J Med Chem 55(22): 9708–9721

Soukup O, Jun D, Zdarova-Karasova J, Patocka J, Musilek K, Korabecny J, Krusek J, Kaniakova M, Sepsova V, Mandikova J, Trejtnar F, Pohanka M, Drtinova L, Pavlik M, Tobin G, Kuca K (2013) A resurrection of 7-MEOTA: a comparison with tacrine. Curr Alzheimer Res 10(8):893–906

Spilovska K, Korabecny J, Kral J, Horova A, Musilek K, Soukup O, Drtinova L, Gazova Z, Siposova K, Kuca K (2013) 7-Methoxytacrine-adamantylamine heterodimers as cholinesterase inhibitors in Alzheimer's disease treatment—synthesis, biological evaluation and molecular modeling studies. Molecules 18(2):2397–2418

Summers WK, Koehler AL, Marsh GM, Tachiki K, Kling A (1989) Long-term hepatotoxicity of tacrine. Lancet 1(8640):729

Tayeb HO, Yang HD, Price BH, Tarazi FI (2012) Pharmacotherapies for Alzheimer's disease: beyond cholinesterase inhibitors. Pharmacol Ther 134(1):8–25

The PyMol Molecular Graphics System. http://www.pymol.org

Tomiyama T, Shoji A, Kataoka K, Suwa Y, Asano S, Kaneko H, Endo N (1996) Inhibition of amyloid beta protein aggregation and neurotoxicity by rifampicin. Its possible function as a hydroxyl radical scavenger. J Biol Chem 271(12):6839–6844

Trott O, Olson AJ (2010) AutoDock Vina: improving the speed and accuracy of docking with a new scoring function, efficient optimization, and multithreading. J Comput Chem 31(2):455–461

Yan A, Wang K (2012) Quantitative structure and bioactivity relationship study on human acetylcholinesterase inhibitors. Bioorg Med Chem Lett 22(9):3336–3342

Yiannopoulou KG, Papageorgiou SG (2013) Current and future treatments for Alzheimer's disease. Ther Adv Neurol Disord 6(1):19–33

Zemek F, Drtinova L, Nepovimova E, Sepsova V, Korabecny J, Klimes J, Kuca K (2014) Outcomes of Alzheimer's disease therapy with acetylcholinesterase inhibitors and memantine. Expert Opin Drug Saf 13(6):759–774

Zheng H, Fridkin M, Youdim M (2014) From single target to multitarget/network therapeutics in Alzheimer's therapy. Pharmaceuticals 7(2):113–135